THE JOURNAL OF BIOLOGICAL CHEMISTRY VOL. 282, NO. 50, pp. 36534–36542, December 14, 2007

Phosphatidylinositol 4-Phosphate 5-Kinase Reduces Cell Surface Expression of the Epithelial Sodium Channel (ENaC) in Cultured Collecting Duct Cells*

Received for publication, May 14, 2007, and in revised form, October 11, 2007 Published, JBC Papers in Press, October 16, 2007, DOI 10.1074/jbc.M703970200

Kelly M. Weixel[‡1], Robert S. Edinger[‡], Lauren Kester[‡], Christopher J. Guerriero[‡2], Huamin Wang[‡], Liang Fang[§], Thomas R. Kleyman[‡], Paul A. Welling[§], Ora A. Weisz[‡], and John P. Johnson[‡3]

From the [‡]Department of Medicine, Renal and Electrolyte Division, University of Pittsburgh, Pittsburgh, Pennsylvania 15261 and the [§]Department of Physiology, University of Maryland School of Medicine, Baltimore, Maryland 21201

Ubiquitination of ENaC subunits has been shown to negatively regulate the cell surface expression of ENaC channels. We have previously demonstrated that epsin links ubiquitinated ENaC to clathrin adaptors for clathrin-mediated endocytosis. Epsin is thought to directly modify the curvature of membranes upon binding to phosphatidylinositol 4,5-bisphosphate (PIP_2) where it recruits clathrin and stimulates lattice assembly. Murine phosphatidylinositol 4-phosphate 5-kinase α (PI5KIα) has been shown to enhance endocytosis in a PIP_2-dependent manner. We tested the hypothesis that PI5KIα-mediated PIP_2 production would negatively regulate ENaC current by enhancing epsin-mediated endocytosis of the channel. Expression of PI5KIα decreased ENaC currents in *Xenopus* oocytes by 80%, entirely because of a decrease in cell surface ENaC levels. Catalytically inactive mutants of PI5Kα had no effect on ENaC activity. Expression of the PIP_2 binding region of epsin increased ENaC current in oocytes, an effect completely reversed by co-expression of PI5KIα. Overexpression of epsin reduced amiloride-sensitive current in CCD cells. Overexpression of PI5KIα enhanced membrane PIP_2 levels and reduced apical surface expression of ENaC in CCD cells, down-regulating amiloride-sensitive current. Knockdown of PI5KIα with isoform-specific siRNA resulted in a 4-fold enhancement of ENaC activity. PI5KIα localized exclusively to the apical plasma membrane domain when overexpressed in mouse CCD cells, consistent for a role in regulating PIP_2 production at the apical plasma membrane. We conclude that membrane turnover events regulating ENaC surface expression and activity in oocytes and CCD cells can be regulated by PI5KIα.

The epithelial sodium channel (ENaC)[4] localizes to the apical plasma membrane of epithelial cells where it functions to regulate Na^+ transport. ENaC activity is critical to the physiological maintenance of Na^+ homeostasis, volume regulation, and thus, systemic blood pressure (1, 2). Because of its central role in responding to extreme changes in Na^+ intake, ENaC transport rates are tightly regulated and defects in the channel or factors regulating the channel result in inherited forms of hypertension and hypotension. Key modulating factors in controlling epithelial Na^+ transport are regulation of the mechanisms that facilitate ENaC surface expression or P_o. ENaC surface expression is regulated by a variety of hormonal and non-hormonal factors, including mineralocorticoids and insulin as well as osmotic changes (2–5). The balance of membrane delivery and retrieval events are coordinated to regulate the number of channels available at the apical membrane for Na^+ reabsorption (6, 7). Indeed, alterations in the removal of ENaC channel from the apical plasma membrane appear to be the underlying cause of Liddle's Syndrome (8). Clearly, identifying the factors that control insertion, retrieval, and recycling of membrane channels will aid in our understanding of the complex action of hormones, physiological and pathological conditions that are associated with altered channel expression or activity.

It is widely accepted that ENaC surface expression is negatively regulated by ubiquitination (9–13). Elegant studies have revealed that the ubiquitin ligase Nedd4-2 binds to a consensus PP*X*Y motif in the C terminus of ENaC subunits and mediates the ubiquitination of lysine residues on the N terminus of the α- and γ-subunits of ENaC in MDCK cells (14, 15). Ubiquitination of membrane proteins serves as a signal for retrieval of these proteins from the cell surface into the endosomal/lysosomal pathway (16). Recently, we demonstrated that ENaC binds to epsin, which facilitates the internalization of ubiquitinated ENaC from the apical plasma membrane of epithelial cells via clathrin-mediated endocytosis (17). Epsin is thought to directly modify the curvature of membranes upon binding to PIP_2 where it recruits clathrin and stimulates lattice assembly (18, 19). The rate of clathrin-mediated endocytosis appears to be influenced by PIP_2 metabolism in a variety of ways. PIP_2 has

* This work was supported in part by Grants DK 57718, DK47874 (to J. P. J.), DK 064613 (to O. A. W.), DK 65161 (to T. S. K.), DK-63049 and DK-54231 (to P. A. W.) from the National Institutes of Health (NIH). The costs of publication of this article were defrayed in part by the payment of page charges. This article must therefore be hereby marked "*advertisement*" in accordance with 18 U.S.C. Section 1734 solely to indicate this fact.
[1] Supported in part by an NIH Institutional National Research Service Award T32 DK61296.
[2] Supported in part by an NIH Institutional National Research Service Award T32 DK61296 and American Heart Association predoctoral fellowship.
[3] To whom correspondence should be addressed: Dept. of Medicine, Renal and Electrolyte Division, University of Pittsburgh, 3500 Terrace St., Pittsburgh, PA 15261. Tel.: 412-648-9075; Fax: 412-383-8956; E-mail: Johnson@dom.pitt.edu.

[4] The abbreviations used are: ENaC, epithelial Na^+ channel; PIP_2, phosphatidylinositol 4,5-bisphosphate; PI5KI, phosphatidylinositol 4-phosphate 5-kinase; HA, hemagglutinin; TLC, thin layer chromatography; BSA, bovine serum albumin; GFP, green fluorescent protein; PBS, phosphate-buffered saline.

been shown to increase the affinity of AP-2 complexes for the internalization signals of a variety of cargo molecules (20). AP-2, which, like epsin, functions to promote clathrin-coated vesicle assembly, also contains PIP_2 selective domains and mutations in the PIP_2 binding regions of epsin or the $\mu 2$ subunit of AP-2 interfere with endocytosis (21, 22).

PIP_2 clearly participates in the regulation of numerous cell processes in addition to endocytosis. Proteins responsible for actin polymerization and cytoskeletal rearrangement are recruited to specific membranes via their interactions with PIP_2 (23, 24). Furthermore, a diverse class of ion channels and transporters can be regulated by direct interaction with PIP_2 and/or are sensitive to dynamic changes in PIP_2 concentrations at the plasma membrane (25). Indeed, PIP_2 has been implicated in the up-regulation of ENaC activity by effects on exocytosis of channels or by direct effects on P_o (26–30).

The versatility assigned to PIP_2 suggests that there are spatially and temporally regulated pools of PIP_2 in the plasma membrane. Generation of PIP_2 at the plasma membrane can be accomplished by the three isoforms of the type I phosphatidylinositol 4-phosphate 5-kinases (PI5Ks) α, β, and γ (31). The mouse and human nomenclature for the α and β isoforms are reversed; for these studies we used the murine cDNA for PI5Kα. With regard to endocytosis, the activity of all three isoforms appears to influence the rate of internalization in various cell types. The assembly of the AP-2 clathrin adaptor complex to the plasma membrane has been shown to be influenced by the activity of both the murine α and γ isoforms of PI5K (32, 33). At the synapse, a very active area of rapid endocytosis, PI5KIγ has been shown to be the predominant enzyme involved in PIP_2 production (34). Interestingly, PIP_2 production via murine PI5KIβ has been shown to increase the regulated process of internalization of EGF receptors, whereas PI5KIα has no effect in fibroblasts (35). Most recently, the direct interaction of type I PI5Ks with AP-2 complexes has been shown to stimulate PI5K activity and the PI5KIγ isoform has been shown to interact with AP-2 complexes and regulate endocytosis of transferrin (33, 36). The majority of these studies were performed in nonpolarized cells or have examined the traffic of basolateral cargo only. It is not clearly known which isoforms are physiologically relevant to apical trafficking in polarized epithelial cells or those which contribute to the balance of ENaC turnover at the apical plasma membrane. The following experiments were designed to test whether modulation of PIP_2 levels via PI5KIα functions to regulate ENaC surface expression and activity in native epithelial cells.

EXPERIMENTAL PROCEDURES

Cell Culture and Adenoviral Expression—mpkCCD$_{c14}$ cells (CCD cells) were derived from the cortical collecting ducts of SV40 transformed mice and were the generous gift of Alain Vandewalle (37). CCD cells were maintained in Dulbecco's modified Eagle's medium/Ham's F12 with 2% fetal bovine serum as previously described. For adenovirus infection, cultured CCD cells were grown on 12-mm transwells (0.4-μm pore; Costar, Cambridge, MA), rinsed extensively with PBS and incubated for 1 h at 37 °C on 50-μl drops of PBS-containing recombinant adenoviruses and 150 μl of PBS/virus on the apical surface of the transwell, using a multiplicity of infection (m.o.i.) of 100. Recombinant adenovirus encoding the constitutive expression of the tetracycline-repressible transactivator at an m.o.i. of 50 was included in all experiments to enable doxycycline-repressible synthesis of appropriate PI5KIα tagged with an HA epitope (38). Following infection, cells were incubated in complete media supplemented with 20 ng/ml doxycycline for 24 h. Subsequently, cells were rinsed in complete media and incubated for 16 h in the absence of doxycycline to allow for expression of PI5KIα constructs. Infection efficiency was visualized by immunofluorescence with anti-HA antibodies and was estimated at greater than 90% for all viruses.

DNA and Replication-defective Recombinant Adenoviruses—The cDNA for murine PI5KIα was kindly provided by Chris Carpenter (Harvard Medical School). This construct was utilized for the generation and purification of replication-defective recombinant adenoviruses (AVs) encoding the tetracycline-repressible construct encoding PI5KIα as described (39). Site-directed mutagenesis to generate the D227A and D203A mutations was performed in the pAdtet PI5KIα cDNA construct by using the QuikChange^{TM} system (Stratagene).

Channel Expression in Xenopus Oocytes—Complementary RNAs (cRNA) for wild-type and mutant constructs were prepared using a cRNA synthesis kit employing T3 RNA polymerase (mMESSAGE mMachine, Ambion Inc, Austin, TX). *Xenopus* oocytes (stage V-VI) were pretreated with 2 mg/ml collagenase (type IV) in calcium-free saline solution. Murine ENaC cRNAs (1–3 ng/subunit in 50 nl of H_20) were microinjected into all oocytes. Oocytes in the experimental group were additionally injected with 5 ng of cRNA of the indicated PI5KIα constructs. All oocytes were incubated at 18 °C in modified Barth's saline (MBS: 88 mM NaCl, 1 mM KCl, 2.4 mM $NaHCO_3$, 0.3 mM $Ca(NO_3)_2$, 0.41 mM $CaCl_2$, 0.82 mM $MgSO_4$, 15 mM HEPES-NaOH, pH 7.2, supplemented with 10 μg/ml sodium penicillin, 10 μg/ml streptomycin sulfate, and 100 μg/ml gentamycin sulfate). Whole cell currents were measured 24–46 h after cRNA injections. Similar experiments were performed using ROMK cRNA (2 ng) injected into oocytes.

Whole Cell Measurements—A two-electrode voltage clamp technique was used as preciously described. Whole cell inward amiloride-sensitive currents were measured in control oocytes expressing $\alpha\beta\gamma$ ENaC alone or experimental oocytes expressing $\alpha\beta\gamma$ ENaC with appropriate PI5KIα constructs using a DigiData 1200 interface (Axon Instruments, Foster City, CA) and a TEV 200A voltage Clamp amplifier (Dagan Corp., Minneapolis, MN). Data acquisition and analysis were performed using pClamp 7.0 (Axon Instruments). Amiloride-sensitive currents were defined as the difference of current in the absence and the presence of 0.1 mM amiloride. Membrane potentials were clamped from −140 to +60 mV in 20-mV increments with duration of 900 ms. Currents were measured at a holding potential of −100 mV, 600 ms after initiation of the clamp potential. For ROMK measurements, oocytes were bathed in a 45 mM K^+ solution (45 mM KCl, 45 mM *N*-methyl-D-glucamine-Cl, 1 mM $MgCl_2$, 1 mM $CaCl_2$, 5 mM HEPES, pH 7.4). Voltage sensing and current injecting microelectrodes had resistances of 0.5–1.5 MΩ when backfilled with 3 M KCl. Once a stable membrane potential was attained, oocytes were

clamped to a holding potential of −20 mV and currents were recorded during 500 ms voltage steps, ranging from −100 mV to +40 mV in 20 mV increments. Data were collected using an ITC16 analog-to-digital, digital-to-analogue converter (Instrutech Corp.), filtered at 1 kHz and digitized on line at 2 kHz using Pulse software (HEKA Electronik) for later analysis. Data shown are based on the average maximum current, measured at −100 mV.

Cell Surface ENaC and ROMK Labeling—Plasma membrane expression of the external HA-tagged ROMK channel and external FLAG-tagged ENaC was measured in single oocytes following procedures outlined as previously reported (40) with slight modifications. In these studies, oocytes were fixed with 4% formaldehyde in oocytes Ringers for 15 min. at 4 °C and washed four times in oocytes Ringers. To block spurious antibody binding, oocytes were then incubated for 1 h at 4 °C in MBS containing 1% bovine serum albumin (BSA). Exposed HA or FLAG epitopes on the surface of intact oocytes were labeled with a rat monoclonal anti-HA antibody (0.5 μg/ml, Roche 3F10, 1% BSA, 4 °C, overnight) or 1 mg/ml mouse monoclonal anti-FLAG antibody (Sigma) for 1 h. Oocytes were washed with MBS containing 1% BSA, and incubated with horseradish peroxidase-coupled goat anti-rat or goat anti-mouse (1 μg/ml, Jackson Laboratories, 1% BSA, 1.5 h). After extensive washing, individual oocytes were placed in chemiluminescence substrate as described (41). Luminescence from single oocytes was measured as described previously (40, 41).

Cell Surface Biotinylation—The cell surface pool of ENaC was determined by surface biotinylation as described (42). Briefly, CCD cells cultured on Transwells were washed (5 min) with ice-cold PBS with agitation on ice to remove growth media. Apical domain selective biotinylation was performed in borate buffer (85 mM NaCl, 4 mM KCl, 15 mM $Na_2B_4O_7$, pH 9) for 20 min. The basolateral surface was incubated in growth medium containing fetal bovine serum (FBS) to prevent biotinylation. The biotinylation was quenched by FBS incubation and PBS washing. Monolayers were lysed (0.4% DCA, 1% Nonidet P-40, 50 mM EGTA, 10 mM Tris-Cl, pH 7.4) at room temperature for 10 min. Protein concentration of the postnuclear supernatant was determined, and 200 μg of protein was combined with a streptavidin bead slurry (Pierce Chemical Co.) and incubated overnight at 4 °C. Samples were collected in 2× sample buffer containing 10% β-mercaptoethanol and incubated for 20 min at room temperature. Samples were SDS-PAGE and Western blot analysis and visualized with enhanced chemiluminescence. Equal concentrations of cell lysate were analyzed in parallel to determine total the total cellular pool of ENaC.

Indirect Immunofluorescence—CCD cells grown on transwell filters were infected with tet-responsive adenoviruses encoding HA epitope-tagged PI5KIα and/or a GFP-tagged PH domain from PLCδ and the tetracycline-repressible transactivator at a m.o.i. 100 as described above. Following infection and expression of the adenovirus, cells were rinsed in PBS and processed for immunofluorescence microscopy. Briefly, the cells were fixed with formaldehyde using a pH-shift protocol as described (43). HA epitope-tagged PI5KIα was visualized using monoclonal anti-HA antibody (1:500) (Covance) and AlexaFluor secondary antibodies (1:500) (Molecular Probes), ZO-1 was visualized using rat anti-ZO-1 hybridoma supernatant R40.76 (1:10) and AlexaFluor secondary antibody (1:500) (Molecular Probes). Images were acquired using a Leica TCL-SL confocal microscope equipped with argon and green and red helium neon lasers (Leica, Dearfield, IL). Images were taken with a 100× (1.4 numerical aperture) plan apochromat oil objective and the appropriate filter combination. The images (1024 × 1024 pixels) were saved in a tag-information-file-format (TIFF), and image contrast was adjusted in the Photoshop program (Adobe, Mountain View, CA).

Thin Layer Chromatography Analysis of Phospholipids—Lipid analysis was performed essentially as described in Ref. 44. *Xenopus* oocytes expressing appropriate cDNAs were incubated overnight with [^{32}P]orthophosphate in modified Barth's media. The following morning samples were washed 1× with modified Barth's to remove unincorporated ^{32}P. Oocytes were homogenized in 300 μl of 1 N HCl, and lipids were extracted as described below. AV-infected CCD cells grown on 6-cm dishes were starved in phosphate-free buffer for 30 min, radiolabeled for 4 h with 40 μCi/ml [^{32}P]orthophosphate (ICN). Cells were rinsed gently in ice-cold buffer and scraped into a 4:3:3 mixture of $CHCl_3$/CH_3OH/1 N HCl. The organic phase was washed with equal volumes of CH_3OH and 1 N HCl. Aliquots were counted using a scintillation counter, and equal counts/min were spotted onto oxalate-treated Silica gel 60 TLC plates (EM Science) and developed in 1-propyl alcohol, 2 M acetic acid; H_2O (63:4:33). Authentic lipid standards (Avanti Polar Lipids) were included in all experiments and visualized using iodine vapor. Radiolabeled products were visualized and quantitated using a phosphorimager (Bio-Rad).

Internalization of IgA—IgA was radioiodinated using the iodine monochloride method as described (45). Endocytosis of ^{125}I-IgA was performed essentially as described by Apodaca *et al.* (46). Briefly, cells were incubated with ^{125}I-IgA applied either to the basolateral or apical surface on ice for 1.5 h. Cells were washed with ice-cold media and incubated in prewarmed 37 °C media in a water bath for appropriate time points. After each time point, ^{125}I-IgA that was not internalized from the cell surface was removed by treating the cells with 25 mg/ml L-1-tosylamide-2-phenylethylchloromethyl-ketone-treated trypsin. The filters were washed and removed from the insert, and the amount of cell-associated ^{125}I-IgA and that which was removed by washing and trypsin treatment were determined using a gamma counter (Packard Instrument, Downers Grove, IL) as described (46). An equal number of mock-infected CCD cells not expressing the pIgR were treated identically to determine nonspecific IgA uptake, and these values were subtracted from those of the pIgR-infected CCD cells. After the final time point, filters were cut out of the insert, and the amount of ^{125}I-IgA in all samples was determined using a gamma counter. An equal number of mock-infected CCD cells not expressing the pIgR were treated identically to determine nonspecific IgA uptake, and these values were subtracted from those of the pIgR-infected CCD cells.

Overexpression of Epsin—Mouse CCD cells were transfected with a Myc-tagged epsin construct (provided by Linton Traub, University of Pittsburgh) using Lipofectamine 2000 standard protocol. The following day, the cells were taken up by trypsin

treatment, pelleted with a brief low speed centrifugation, and plated on 12-mm filter inserts (Transwells) at superconfluency. Two days later, the cells were used for electrophysiological or biochemical measurements.

siRNA of PIP5Kα—Approximately 2×10^6 of 80–90% confluent cells were resuspended in nucleofector T solution and 2 pmol (final concentration) of siRNA specific for PI5K Iα (Dharmacon), mixed in the cuvette and directly placed in the nucleofector device (Amaxa Biosystems). The siRNA oligonucleotides were electroporated into the cells using program K-29. An equal volume of warm culture media was added, and the cell suspension plated on a plastic 12-well plate containing 2 ml of culture media. The following day, the cells were trypsinized and plated on 12-mm filter inserts (Transwells) at superconfluency. Two days later, the cells were used for electrophysiological or biochemical study.

RESULTS

The effect of PI5KIα-mediated PIP_2 production on ENaC activity was initially examined using the *Xenopus* oocyte expression system. To determine to what extent PIP_2 production was modified in oocytes expressing PI5KIα, lipids were extracted from oocytes injected with PI5KIα or control cRNAs and examined by thin layer chromatography. As shown in Fig. 1*A* PI5KIα induced a 40% increase in steady state PIP_2 production in oocytes compared with control. Whole cell amiloride-sensitive currents were measured in oocytes coinjected with cRNAs for αβγ ENaC and PI5KIα. Co-expression of PI5KIα with αβγ ENaC reduced amiloride-sensitive current by 80% (Fig. 1*B*). To confirm that the effect of PI5KIα on ENaC surface activity is due to modulation of PIP_2 production, we examined the effect of catalytically inactive mutants $PI5KI\alpha_{D227A}$ (47) and $PI5KI\alpha_{D203A}$[5] on ENaC activity in *Xenopus* oocytes. Co-expression of either mutant with ENaC has no effect on amiloride-sensitive currents compared with control oocytes expressing ENaC subunits alone (Fig. 1*B*), indicating that the catalytic activity of PI5KIα is necessary for the down-regulation of ENaC channel activity.

PIP_2 has been shown to enhance endocytic and exocytic events to control steady state levels of proteins in the plasma membrane. To determine whether the PI5KIα-mediated reduction in ENaC activity is caused by differences in cell surface expression, plasma membrane-associated ENaC channels were examined using an enzyme-linked luminescence assay (40). The surface expression signal of externally FLAG epitope-tagged ENaC was roughly 10-fold higher than the background level of oocytes expressing the wild-type ENaC lacking an external FLAG epitope (Fig. 1*C*, αβγ *versus* $\alpha\beta_{flag}\gamma$). Co-expression of PI5KIα with $\alpha\beta_{flag}\gamma$ ENaC reduced the surface signal of ENaC by nearly 6-fold (Fig. 1*C*) correlating with the reduction observed in amiloride-sensitive current in Fig. 1*A*. These data demonstrate that the reduction of ENaC activity by PI5KIα is caused by an effect on surface density. This negative effect of PIP_2 production on ENaC activity and surface expression is consistent with the role of PIP_2 in enhancing retrieval of ENaC from the plasma membrane.

[5] C. Carpenter, personal communication.

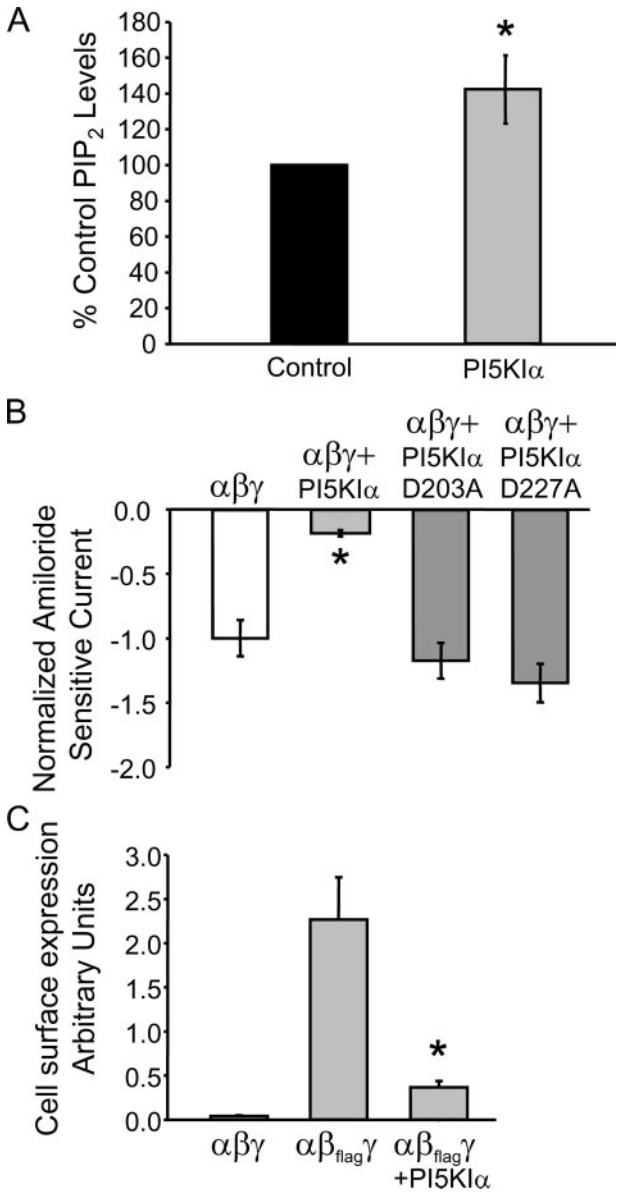

FIGURE 1. **Effect of PI5KIα on ENaC activity and surface expression.** *Panel A*, PI5KIα expression up-regulates PIP_2 production in oocytes. Oocytes injected with cRNA for PI5KIα were ^{32}P-labeled overnight subject to lipid extraction. Equal counts of lipids were resolved by TLC and quantified by phosphorimage analysis. Averages of PIP_2 levels from oocytes expressing PI5KIα are graphed relative to the control (C = 100), $n = 3$. *Panel B*, PI5KIα-mediated PIP_2 production reduces amiloride-sensitive currents in oocytes expressing ENaC subunits. *Xenopus* oocytes were co-injected with the cRNAs for αβγ ENaC and the indicated type I PI5K. Whole cell amiloride-sensitive currents were measured 24–46 h post-injection. Co-expression of wild-type PI5KIα reduced amiloride-sensitive currents by 80% while expression of catalytically inactive mutants $PI5KI\alpha_{D227A}$ or $PI5KI\alpha_{D203A}$ had no effect on ENaC channel activity. Results are normalized to control currents. $n = 18–32$; *, $p < 0.001$ compared with control. *Panel C*, PI5KIα reduces cell surface expression of ENaC in *Xenopus* oocytes. *Xenopus* oocytes were co-injected with external FLAG epitope-tagged β-ENaC with wild-type α and γ ($\alpha\beta_{flag}\gamma$) alone or in combination with PI5KIα. Wild-type αβγ lacking FLAG epitope-tagged β (αβγ) is expressed as control for background. Cell surface expression of FLAG-tagged ENaC was analyzed by luminometry as described under "Experimental Procedures." Co-expression of PI5KIα reduced the surface expression of epitope-tagged ENaC nearly 6-fold. $n = 25$. $p < 0.001$ compared with $\alpha\beta_{flag}\gamma$.

Type I PI5Ks have been shown to produce specific pools of PIP_2 that can be utilized for distinct membrane trafficking events (34, 48, 49). To determine whether PI5KIα-mediated

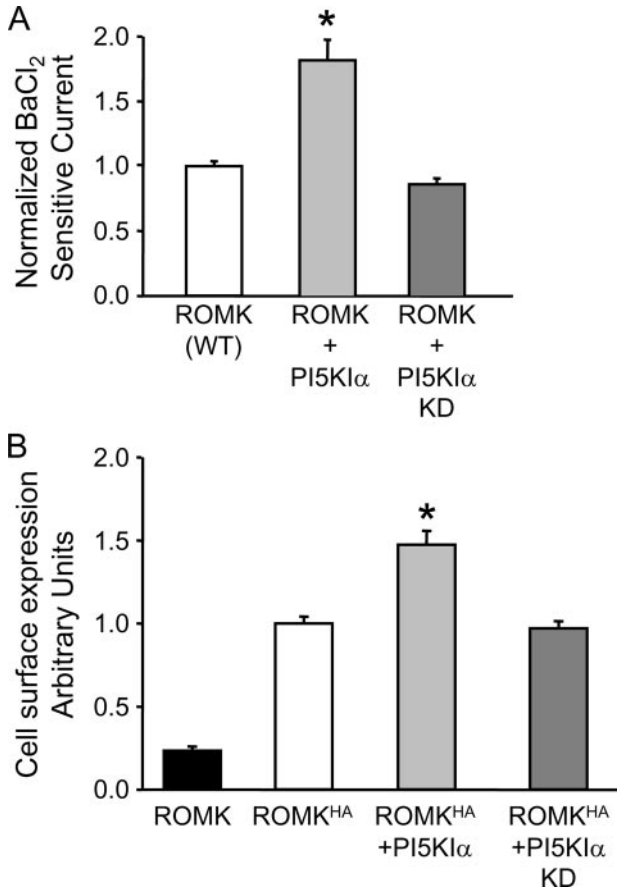

FIGURE 2. **PI5KIα up-regulates ROMK activity and surface expression in oocytes.** *Panel A*, *Xenopus* oocytes were injected with cRNA encoding ROMK alone or in combination with PI5KIα cRNA. Voltage-sensing and current-injecting microelectrodes had resistances of 0.5–1.5 MΩ when backfilled with 3 M KCl. Once a stable membrane potential was attained, oocytes were clamped to a holding potential of −20 mV and currents were recorded during 500-ms voltage steps, ranging from −100 mV to +40 mV in 20-mV increments. Data shown are based on the average maximum current, measured at −100 mV. *Panel B*, cell surface expression of HA-tagged ROMK channel was measured in single oocytes as described under "Experimental Procedures."

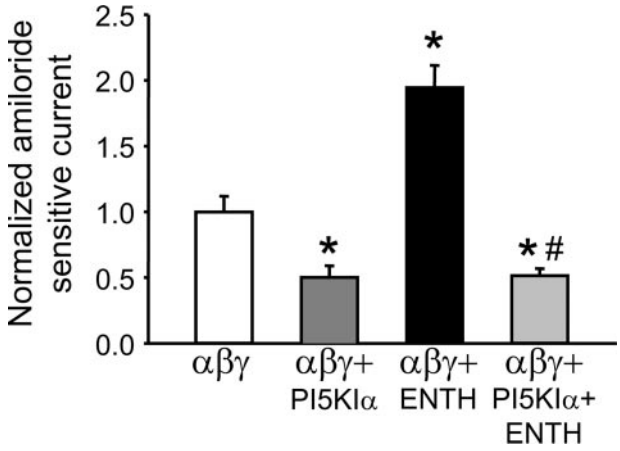

FIGURE 3. **PI5KIα blocks ENTH domain-stimulated ENaC current.** *Xenopus* oocytes were co-injected with cRNAs encoding αβγ subunits of ENaC alone or in combination with cRNA for PI5KIα and/or the ENTH domain of epsin as described under "Experimental Procedures." Whole cell currents were measured 24 h later. Co-expression of PI5KIα with the ENTH domain reduced amiloride-sensitive currents to below control ENaC currents. $n = 25$; *, $p < 0.002$ compared with control. #, $p < 0.001$ compared with αβγ + ENTH.

PIP_2 production is important for constitutive trafficking and steady state distribution of other membrane proteins, we tested the effect of PI5KIα on the activity and surface expression of the renal potassium secretory channel, ROMK. Interestingly, PI5KIα expression enhanced ROMK activity in oocytes (Fig. 2*A*). This effect was dependent upon PIP_2 production, as catalytically inactive mutants had no effect on ROMK activity (Fig. 2*A*). Furthermore, PI5KIα induced a 50% increase in ROMK surface expression in oocytes as detected by luminometry, indicating that the up-regulation in ROMK activity is caused by increased levels of ROMK channels at the membrane (Fig. 2*B*). These observations suggest that the PI5KIα-mediated effects on ENaC surface expression may be related to specific protein-protein interactions relevant to ENaC internalization.

We have previously shown that the adaptor protein epsin, which contains an N-terminal PIP_2 binding ENTH domain, functions in the retrieval of ubiquitinated ENaC from the plasma membrane (17). Co-expression of the epsin ENTH domain with ENaC subunits in *Xenopus* oocytes results in increased current compared with currents obtained upon expression of ENaC subunits alone. We hypothesized that expression of this domain sequesters PIP_2 at the plasma membrane, thereby inhibiting endocytosis. To test this, we examined whether enhancing levels of PIP_2 through co-expression of PI5KIα would block ENTH domain-mediated stimulation of ENaC current. Indeed, PI5KIα reversed the effect we observed with the ENTH domain alone by reducing amiloride-sensitive currents to below control levels in oocytes, (Fig. 3).

As noted above, the underlying hypothesis of this work is that ENaC subunits, ubiquitinated at the plasma membrane (11–13) is linked to clathrin adaptors by epsin, which in turn recruits PIP_2 to the complex, facilitating internalization via clathrin-mediated endocytosis. Although our data in oocytes, along with data by ourselves and others (11, 12, 50) indicating interactions between ENaC and clathrin adaptors, tend to support this model, we next sought to examine this directly in CCD cells that endogenously express ENaC. We first examined the effects of overexpression of epsin and PI5KIα on ENaC activity in CCD cells. As shown in Fig. 4*A*, both proteins induce a substantial and virtually identical reduction in ENaC current in CCD cells. To examine the functional role of the pool of PIP_2 generated by PI5KIα on native ENaC channels we determined whether expression of wild-type PI5KIα would raise PIP_2 production in CCD membranes. Following infection, cells were labeled with [^{32}P]orthophosphate, lipids extracted, and analyzed by TLC (Fig. 4*B*). Overexpression of PI5KIα more than doubled the amount of PIP_2 produced in CCD cells compared with control infected cells. Transepithelial amiloride-sensitive currents were measured in parallel experiments to determine the effect of enhanced PIP_2 production via PI5KIα in CCD cells. Fig. 4*A* demonstrates that enhanced PIP_2 production resulted in a significant reduction in ENaC activity, consistent with the effects observed in *Xenopus* oocytes (Fig. 1*B*). Furthermore, the expression of the catalytically inactive mutants $PI5KI\alpha_{D227A}$ of $PI5K1\alpha_{D203A}$ had no effect on the amiloride-sensitive current in CCD cells compared with control (Fig. 4*C*). Next, we determined whether this effect was caused by changes in ENaC sur-

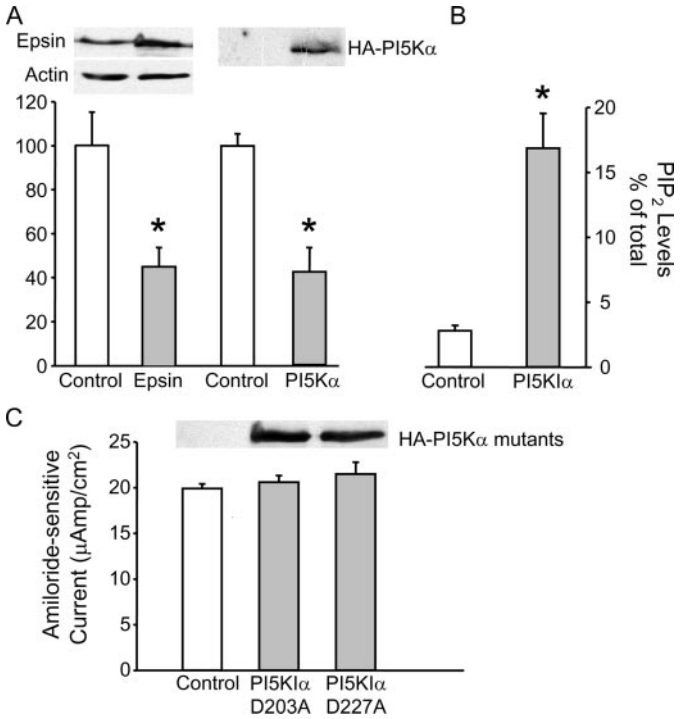

FIGURE 4. **Effects of epsin and PI5KIα overexpression on ENaC activity in CCD cells and effects of PI5KIα on PIP_2 levels.** *Panel A*, effects of PI5KIα on ENaC activity in CCD cells. CCD cells were infected with adenovirus encoding catalytically inactive PI5KIα constructs or control or transfected with HA-epsin under a constitutive promoter as described under "Experimental Procedures." Amiloride sensitive short-circuit current was measured 24 h after induction. *Panel B*, following adenovirus infection, cells were labeled for 4 h with [^{32}P]orthophosphate, and their lipids were extracted and examined by TLC. The mean PIP_2 levels in cells infected with PI5KIα or control adenovirus in two experiments performed in duplicate are graphed. $p < 0.001$. *Panel C*, CCD cells were infected with adenovirus encoding HA-tagged catalytically inactive mutants of PI5KIα or a control constructs. Amiloride-sensitive short-circuit current was measured 24 h after induction. *Inset* shows equal expression of HA tag with both viruses. $n = 6$; $p < 0.002$.

face expression. The steady state levels of ENaC expressed at the surface were determined by domain-selective cell surface biotinylation as described under "Experimental Procedures." The total cellular pool of ENaC channels was unchanged by PI5KIα expression in immunoblots of CCD lysates probed with anti-α ENaC antibodies, (Fig. 5*A*, *top panel*). However, cell surface biotinylation of polarized CCD cells demonstrate that the amount of ENaC expressed at the cell surface was reduced by 60% in cells expressing PI5KIα compared with control, Fig. 5*A*, *bottom panel* and Fig. 5*B*). These observations are consistent with the role of PIP_2 in promoting internalization events at the plasma membrane. If this is correct, then knockdown of PI5KIα in CCD cells should inhibit internalization, as it did in non-polarized cells (32), and potentially result in increased ENaC activity. As shown in Fig. 6*B*, CCD cells express all three isoforms of Type I PI5K. To knockdown expression of the specific isoform which we had previously overexpressed, CCD cells were treated with small interfering RNA (siRNA) constructs specific for the Iα isoform of murine PI5K. ENaC currents and abundance of PI5KIα were measured 2 days later. As shown in Fig. 6*A*, treatment of the cells resulted in substantial reduction in expression of the kinase and a 4-fold enhancement of amiloride-sensitive current.

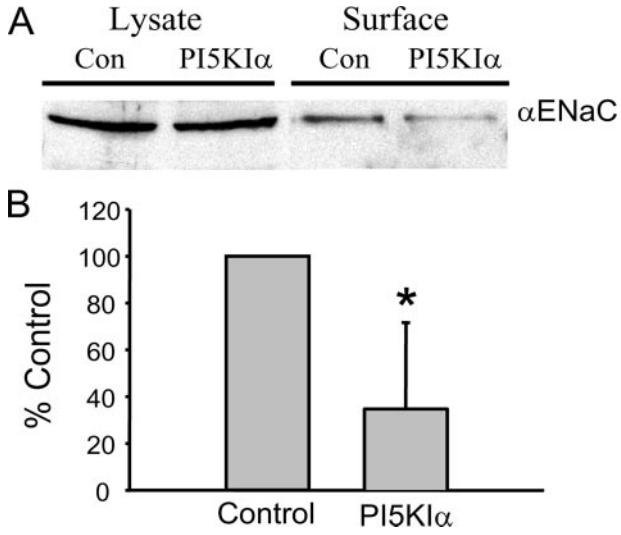

FIGURE 5. **PI5KIα overexpression reduces cell surface expression of native ENaC in CCD cells.** CCD cells were infected with control or PI5KIα adenovirus and subject to cell surface biotinylation. Biotinylated proteins were recovered by streptavidin and examined by Western blot analysis with anti-α-ENaC antibodies. *Panel A*, equal concentrations of cell lysate were analyzed in parallel to determine total the total cellular pool of α-ENaC, *Panel B*, quantification of cell surface expression of α-ENaC in control and PI5KIα-expressing CCD cells. $n = 3$; $p = 0.038$.

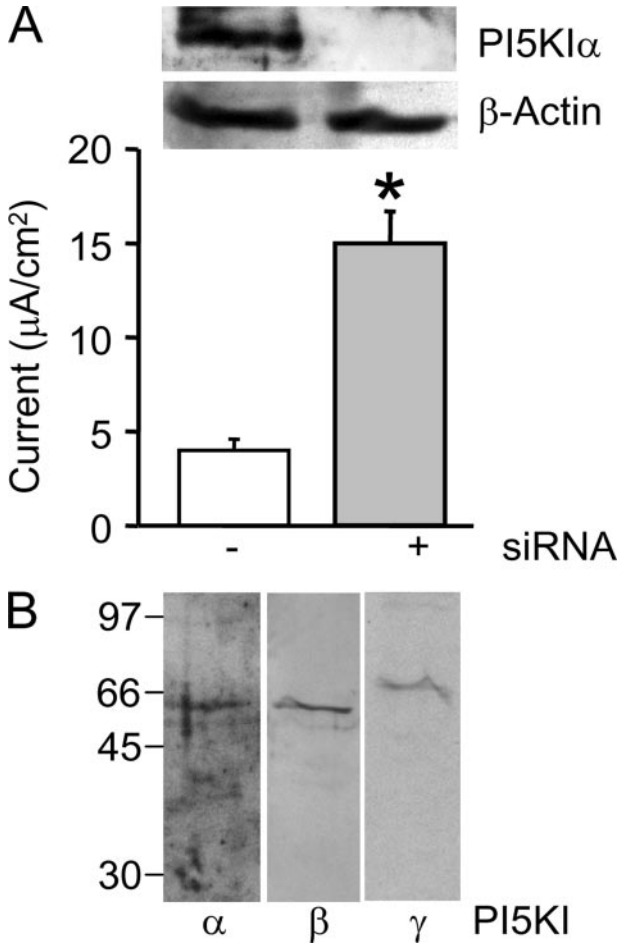

FIGURE 6. **Effect of knockdown of PI5KIα on ENaC activity in CCD cells.** *Panel A*, isoform-specific siRNA directed against PI5KIα introduced into CCD cells as described under "Experimental Procedures" and amiloride-sensitive current was measured 2 days later. *Inset* shows the effect of siRNA on PI5KIα abundance by Western blot. $n = 3$; *, $p < 0.001$. *Panel B*, equal concentrations of CCD cell lysate were blotted for the three specific Type I PI5K isoforms.

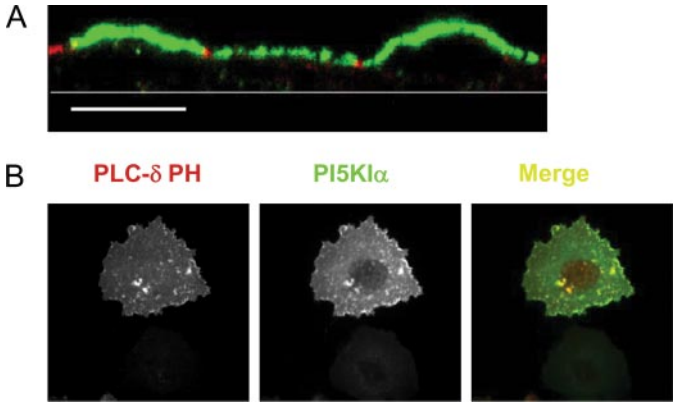

FIGURE 7. **PI5KIα segregates to the apical plasma membrane in polarized CCD cells.** *Panel A*, PI5KIα localizes to the apical membrane of polarized CCD cells. CCD cells infected with adenovirus encoding PI5KIα were immunolabeled with antibodies against HA epitope tag in PI5KIα (*green*) and the tight junction marker, Zo-1 (*red*). The overexpressed isoform discretely localizes to the apical plasma membrane. Images are representative of multiple fields examined in 2 separate filters. *Scale bar*, 5 μm. *Line* indicates position of the filter. *Panel B*, PI5KIα localizes to the plasma membrane in nonpolarized cells. Nonpolarized CCD cells were infected with PI5KIα and GFP-PLCδ-PH adenoviruses and processed for immunofluorescence as described under "Experimental Procedures." PI5KIα distributes to the plasma membrane with GFP-PLCδ-PH. *Scale bar*, 10 μm.

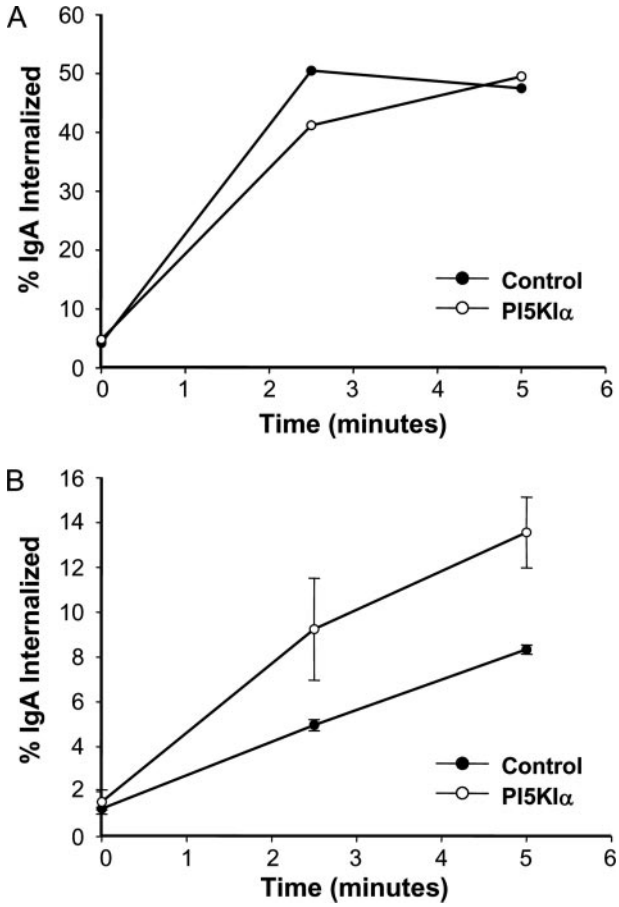

FIGURE 8. **Effect of PI5KIα on polarized endocytic traffic in CCD cells.** *Panel A*, basolateral ^{125}I-IgA endocytosis is unaffected by PI5KIα activity in polarized CCD cells. Basolateral uptake of ^{125}I-IgA was monitored in CCD cells infected with control or PI5KIα as described under "Experimental Procedures." A representative graph of three experiments is shown. *Panel B*, PI5KIα stimulates ^{125}I-IgA endocytosis in nonpolarized CCD cells. Subconfluent CCD cells grown on plastic were infected with control or PI5KIα adenovirus. ^{125}I-IgA internalization was monitored over time as described under "Experimental Procedures." Data are means ± S.E. of three experiments.

We next examined the localization of PI5KIα in polarized and nonpolarized CCD cells. Cells were infected with HA epitope-tagged PI5KIα and processed for immunofluorescence 16 h after induction of expression. PI5KIα was highly enriched in the apical plasma membrane of polarized CCD cells as assessed by confocal microscopy. In xzy sections of CCD cells, PI5KIα (*green*, Fig. 7*A*) localizes predominantly at the apical membrane and does not stain the lateral borders, delineated by antibodies staining the junctional marker, Zo-1 (*red*, Fig. 7*A*). When CCD cells are grown subconfluently on glass coverslips, PI5KIα localizes predominantly at the plasma membrane (*red*, Fig. 7*B*) where it localizes with the PIP_2-binding PH domain from PLCδ (*green*, Fig. 7*B*) as reported in the literature (32). PI5KIα also can be found on intracellular structures in nonpolarized epithelial cells (Fig. 7*B*), consistent with previous studies (39).

The reduced pool of ENaC at the cell surface in PI5KIα cells prohibited experiments to determine the kinetics of internalization. Therefore, we examined the effect of PI5KIα on the internalization of IgA and its receptor, the polymeric immunoglobulin receptor (pIgR) in polarized CCD cells. CCD cells were co-infected with adenoviruses encoding pIgR and either PI5KIα or control adenoviruses. ^{125}I-IgA was prebound to pIgR molecules at the basolateral surface at 4 °C, the cells were warmed to 37 °C for the indicated times and cell associated ^{125}I-IgA was quantified in a gamma counter as described under "Experimental Procedures." As shown in Fig. 8*A*, the percent of IgA internalized from the basolateral surface was unaltered by overexpression of PI5KIα. Similar experiments were conducted to follow the internalization of IgA from the apical domain, which has been reported in other cell lines. However, apical endocytosis of this ligand was virtually undetectable in CCD cells, and the results could not be reliably interpreted. PI5KIα has previously been shown to affect rates of internalization in nonpolarized cells (32), thus, we measured ^{125}I-IgA endocytosis in nonpolarized CCD cells infected with pIgR and PI5KIα or control adenoviruses. In contrast to our observations in polarized cells, IgA endocytosis was dramatically stimulated in nonpolarized cells, Fig. 8*B*. These results indicate that the pool of PIP_2 produced by PI5KIα is further compartmentalized in polarized cells, and selectively regulates internalization at the apical surface.

DISCUSSION

Here we have tested the role of PI5KIα on regulating the surface expression of ENaC. We show that PI5KIα down-regulated ENaC activity in *Xenopus* oocytes. The decrease in ENaC activity was dependent on the production of PIP_2, as PI5KIα mutants defective in catalytic activity had no effect. This observation could be reproduced in CCD cells which natively express ENaC, indicating that the mechanism for PI5KIα-mediated down-regulation is preserved in a polarized epithelial cell model. Furthermore, a parallel decrease in surface expression with ENaC activity is observed in oocytes and in polarized CCD cells co-expressing PI5KIα (Fig. 1, *A* and *C* and Fig. 4). Consistent with these observations, knockdown of PI5KIα by siRNA

resulted in striking increase in ENaC activity in CCD cells. Interestingly, the effects of this kinase on ENaC activity were not due to global changes in membrane internalization, as activity and expression of ROMK in oocytes was enhanced, consistent with an effect on exocytosis of this channel (Fig. 2, *A* and *B*). These observations indicate that the influence of PI5KIα on ENaC activity and surface expression may be caused by the interactions required for ENaC internalization. We have previously shown that ubiquitinated ENaC interacts with epsin to promote its internalization through clathrin-coated vesicles (17). Epsin recruitment is PIP_2-dependent; therefore, it is likely that PI5KIα effects are caused by modulating epsin-PIP_2 interactions through the ENTH domain in epsin. Indeed, we observed that while the expression of ENTH domain alone stimulated ENaC current in oocytes, this could be reversed by co-expressing ENTH and PI5KIα with ENaC subunits. These data indicate that the ENTH-PIP_2 interactions can be modulated by PI5KIα and that this pool of PIP_2 is important for the effects we observe on ENaC activity.

The ability of PIP_2 to recruit clathrin-accessory proteins appears to have a rate-limiting effect on constitutive endocytosis. Generation of PIP_2 at the plasma membrane is regulated by the type I PI5Ks, all three of which have documented roles in regulating clathrin-mediated endocytosis. The production of PIP_2 via PI5KIα increases recruitment of the clathrin adaptor complex, AP-2, to the plasma membrane with a coordinate increase in endocytosis of the transferrin receptor in nonpolarized cells, whereas the β isoform has a similar effect on EGF receptor endocytosis in NR6 cells (32). Additionally, PI5KIγ interacts directly with AP-2 *in vitro* and *in vivo* in HEK293 cells, suggesting a mechanism for selective generation of PIP_2 at sites of endocytosis. The γ isoform has also been shown to be responsible for the generation of PIP_2 at synaptic nerve terminals. These studies indicate that individual isoforms can be involved in selective trafficking events in specific cell types. The function and spatial organization of these individual isoforms has not been well described in polarized epithelial cells, which compartmentalize their plasma membrane into apical and basolateral domains. Recent studies have demonstrated a role for PI5KIα in regulating the transport of newly synthesized proteins to the apical surface of MDCK cells, while PI5KIγ functions to regulate the endocytosis of transferrin at the basolateral surface of MDCK cells (33, 39). These observations indicate a role for the compartmental organization of specific Type I PI5K isoforms in regulating PIP_2 at distinct membrane domains.

The localization of PI5KIα to the apical surface of CCD cells (Fig. 7*A*) also argues for its role in regulating membrane events at the apical domain of polarized cells. Consistent with this is our observation that IgA endocytosis from the basolateral domain is unaffected by this up-regulation in PIP_2 production via PI5KIα in polarized CCD cells (Fig. 8*A*). However, when PI5KIα is expressed in nonpolarized CCD cells, where it localizes uniformly to the plasma membrane, it stimulates IgA internalization, consistent with the described function of this enzyme in other nonpolarized cell models (Fig. 8*B*). Interestingly, recent studies have shown that PI5KIγ localizes to basolateral membranes in polarized MDCK cells and regulates trafficking events at this membrane domain (33, 51). Taken together, these studies demonstrate that the spatial organization of PI5K isoforms contributes to the functional specificity of PIP_2 production in membrane trafficking.

PIP_2 has been shown to influence the activity of ENaC via changes in open probability by direct interactions with the channel such that increases in PIP_2 concentration increase activity or prevent rundown in excised patch experiments (26, 28, 30). This points to a different type of local regulation of ENaC via PIP_2 much like that described for GIRK channels, which are down-regulated in parallel with local depletions in PIP_2. Therefore, a local increase in PIP_2 might be expected to enhance ENaC activity, perhaps in an acute manner. While PIP_2 has previously been shown to increase ENaC channel density in the membrane, these studies utilized the murine β isoform of type I PI5K (27, 29), therefore, it is likely that the influence of PIP_2 on ENaC can be independently regulated by different isoforms of PI5K. Additionally, the isoforms of PI5KI are segregated in polarized epithelial cells, presumably to allow for independent modulation of PIP_2 production at different surface domains. Moreover, prolonged up-regulation of PIP_2 production could impact multiple pathways that affect channel number or cell surface residence time. Taken together, these data demonstrate that ENaC channel activity can be negatively regulated by the production of PIP_2 via PI5KIα, likely through its effects on specific endocytic events at the apical membrane of polarized epithelial cells. Thus, PIP_2 appears to have both a positive and negative regulatory role in ENaC function in polarized renal epithelial cells, and this is maintained by spatially modulated metabolism of PIP_2.

Acknowledgments—We thank Tamas Balla and Chris Carpenter for their generous gifts of reagents.

REFERENCES

1. Swift, P. A., and MacGregor, G. A. (2004) *Am. J. Pharmacogenomics* **4,** 161–168
2. Rossier, B. C., Pradervand, S., Schild, L., and Hummler, E. (2002) *Annu. Rev. Physiol.* **64,** 877–897
3. Eaton, D. C., Malik, B., Saxena, N. C., Al-Khalili, O. K., and Yue, G. (2001) *J. Membr. Biol.* **184,** 313–319
4. Flores, S. Y., Debonneville, C., and Staub, O. (2003) *Pflugers Arch.* **446,** 334–338
5. Ma, H. P., and Eaton, D. C. (2005) *J. Am. Soc. Nephrol.* **16,** 3182–3187
6. Snyder, P. M. (2002) *Endocr. Rev.* **23,** 258–275
7. Snyder, P. M. (2005) *Endocrinology* **146,** 5079–5085
8. Rotin, D., Kanelis, V., and Schild, L. (2001) *Am. J. Physiol. Renal Physiol.* **281,** F391–F399
9. Snyder, P. M., Olson, D. R., and Thomas, B. C. (2002) *J. Biol. Chem.* **277,** 5–8
10. Zhou, R., and Snyder, P. M. (2005) *J. Biol. Chem.* **280,** 4518–4523
11. Lu, C., Pribanic, S., Debonneville, A., Jiang, C., and Rotin, D. (2007) *Traffic* **8,** 1246–1264
12. Wiemuth, D., Ke, Y., Rohlfs, M., and McDonald, F. J. (2007) *Biochem. J.* **405,** 147–155
13. Zhou, R., Patel, S. V., and Snyder, P. M. (2007) *J. Biol. Chem.* **282,** 20207–20212
14. Rotin, D., Staub, O., and Haguenauer-Tsapis, R. (2000) *J. Membr. Biol.* **176,** 1–17
15. Malik, B., Yue, Q., Yue, G., Chen, X., Price, S. R., Mitch, W. E., and Eaton, D. C. (2005) *Am. J. Physiol. Renal Physiol*
16. Raiborg, C., Rusten, T. E., and Stenmark, H. (2003) *Curr. Opin. Cell Biol.*

15, 446–455
17. Wang, H., Traub, L. M., Weixel, K. M., Hawryluk, M. J., Shah, N., Edinger, R. S., Perry, C. J., Kester, L., Butterworth, M. B., Peters, K. W., Kleyman, T. R., Frizzell, R. A., and Johnson, J. P. (2006) *J. Biol. Chem.* **281,** 14129–14135
18. Ford, M. G., Mills, I. G., Peter, B. J., Vallis, Y., Praefcke, G. J., Evans, P. R., and McMahon, H. T. (2002) *Nature* **419,** 361–366
19. Ford, M. G., Pearse, B. M., Higgins, M. K., Vallis, Y., Owen, D. J., Gibson, A., Hopkins, C. R., Evans, P. R., and McMahon, H. T. (2001) *Science* **291,** 1051–1055
20. Rapoport, I., Miyazaki, M., Boll, W., Duckworth, B., Cantley, L. C., Shoelson, S., and Kirchhausen, T. (1997) *EMBO J.* **16,** 2240–2250
21. Rohde, G., Wenzel, D., and Haucke, V. (2002) *J. Cell Biol.* **158,** 209–214
22. Itoh, T., Koshiba, S., Kigawa, T., Kikuchi, A., Yokoyama, S., and Takenawa, T. (2001) *Science* **291,** 1047–1051
23. Sakisaka, T., Itoh, T., Miura, K., and Takenawa, T. (1997) *Mol. Cell. Biol.* **17,** 3841–3849
24. Shibasaki, Y., Ishihara, H., Kizuki, N., Asano, T., Oka, Y., and Yazaki, Y. (1997) *J. Biol. Chem.* **272,** 7578–7581
25. Hilgemann, D. W., Feng, S., and Nasuhoglu, C. (2001) *Sci. STKE.* 2001, RE19
26. Yue, G., Malik, B., Yue, G., and Eaton, D. C. (2002) *J. Biol. Chem.* **277,** 11965–11969
27. Staruschenko, A., Nichols, A., Medina, J. L., Camacho, P., Zheleznova, N. N., and Stockand, J. D. (2004) *J. Biol. Chem.* **279,** 49989–49994
28. Kunzelmann, K., Bachhuber, T., Regeer, R., Markovich, D., Sun, J., and Schreiber, R. (2005) *FASEB J.* **19,** 142–143
29. Pochynyuk, O., Medina, J., Gamper, N., Genth, H., Stockand, J. D., and Staruschenko, A. (2006) *J. Biol. Chem.* **281,** 26520–26527
30. Pochynyuk, O., Tong, Q., Staruschenko, A., Ma, H. P., and Stockand, J. D. (2006) *Am. J. Physiol. Renal Physiol.* **290,** F949–F957
31. Blazer-Yost, B. L., Butterworth, M., Hartman, A. D., Parker, G. E., Faletti, C. J., Els, W. J., and Rhodes, S. J. (2001) *Am. J. Physiol. Cell Physiol.* **281,** C624–C632
32. Padron, D., Wang, Y. J., Yamamoto, M., Yin, H., and Roth, M. G. (2003) *J. Cell Biol.* **162,** 693–701
33. Bairstow, S. F., Ling, K., Su, X., Firestone, A. J., Carbonara, C., and Anderson, R. A. (2006) *J. Biol. Chem.* **281,** 20632–20642
34. Wenk, M. R., Pellegrini, L., Klenchin, V. A., Di, P. G., Chang, S., Daniell, L., Arioka, M., Martin, T. F., and De, C. P. (2001) *Neuron* **32,** 79–88
35. Barbieri, M. A., Heath, C. M., Peters, E. M., Wells, A., Davis, J. N., and Stahl, P. D. (2001) *J. Biol. Chem.* **276,** 47212–47216
36. Krauss, M., Kukhtina, V., Pechstein, A., and Haucke, V. (2006) *Proc. Natl. Acad. Sci. U. S. A.* **103,** 11934–11939
37. Bens, M., Vallet, V., Cluzeaud, F., Pascual-Letallec, L., Kahn, A., Rafestin-Oblin, M. E., Rossier, B. C., and Vandewalle, A. (1999) *J. Am. Soc. Nephrol.* **10,** 923–934
38. Henkel, J. R., Apodaca, G., Altschuler, Y., Hardy, S., and Weisz, O. A. (1998) *Mol. Biol. Cell* **9,** 2477–2490
39. Guerriero, C. J., Weixel, K. M., Bruns, J. R., and Weisz, O. A. (2006) *J. Biol. Chem.* **281,** 15376–15384
40. Lebowitz, J., Edinger, R. S., An, B., Perry, C. J., Onate, S., Kleyman, T. R., and Johnson, J. P. (2004) *J. Biol. Chem.* **279,** 41985–41990
41. Yoo, D., Kim, B. Y., Campo, C., Nance, L., King, A., Maouyo, D., and Welling, P. A. (2003) *J. Biol. Chem.* **278,** 23066–23075
42. Butterworth, M. B., Edinger, R. S., Johnson, J. P., and Frizzell, R. A. (2005) *J Gen. Physiol.* **125,** 81–101
43. Leung, S. M., Rojas, R., Maples, C., Flynn, C., Ruiz, W. G., Jou, T. S., and Apodaca, G. (1999) *Mol. Biol. Cell* **10,** 4369–4384
44. Bruns, J. R., Ellis, M. A., Jeromin, A., and Weisz, O. A. (2002) *J. Biol. Chem.* **277,** 2012–2018
45. Breitfeld, P. P., Casanova, J. E., Harris, J. M., Simister, N. E., and Mostov, K. E. (1989) *Meth. Cell Biol.* **32,** 329–337
46. Apodaca, G., Katz, L. A., and Mostov, K. E. (1994) *J. Cell Biol.* **125,** 67–86
47. Tolias, K. F., Hartwig, J. H., Ishihara, H., Shibasaki, Y., Cantley, L. C., and Carpenter, C. L. (2000) *Curr. Biol.* **10,** 153–156
48. Coppolino, M. G., Dierckman, R., Loijens, J., Collins, R. F., Pouladi, M., Jongstra-Bilen, J., Schreiber, A. D., Trimble, W. S., Anderson, R., and Grinstein, S. (2002) *J. Biol. Chem.* **277,** 43849–43857
49. Ling, K., Bairstow, S. F., Carbonara, C., Turbin, D. A., Huntsman, D. G., and Anderson, R. A. (2007) *J. Cell Biol.* **176,** 343–353
50. Staruschenko, A., Pochynyuk, O., and Stockand, J. D. (2005) *J. Biol. Chem.* **280,** 39161–39167
51. Kleyman, T. R., Smith, P. R., and Benos, D. J. (1994) *Am. J. Physiol.* **266,** C1105–C1111